

# **Materials Technology**



Advanced Performance Materials

ISSN: (Print) (Online) Journal homepage: www.tandfonline.com/journals/ymte20

# The global contribution of crystal boundaries and bio-physical characteristics in the understanding of cellular interaction of fibroblasts with the nanoscale surface

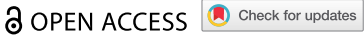
R.D.K. Misra & A. Enchinton

**To cite this article:** R.D.K. Misra & A. Enchinton (2024) The global contribution of crystal boundaries and bio-physical characteristics in the understanding of cellular interaction of fibroblasts with the nanoscale surface, Materials Technology, 39:1, 2326331, DOI: 10.1080/10667857.2024.2326331

To link to this article: <a href="https://doi.org/10.1080/10667857.2024.2326331">https://doi.org/10.1080/10667857.2024.2326331</a>









# The global contribution of crystal boundaries and bio-physical characteristics in the understanding of cellular interaction of fibroblasts with the nanoscale surface

R.D.K. Misra and A. Enchinton

Department of Metallurgical, Materials, and Biomedical Engineering, University of Texas at El Paso, 500 West University Avenue, El Paso,

#### **ABSTRACT**

The primary objective here is to underscore the significance of high percentage of crystal boundaries (>50%) of a nanocrystalline (NC) surface in understanding the cellular interaction of fibroblasts with the NC surface of biomedical stainless steel. The favourable cellular functions on the NC surface as compared to the conventional microcrystalline (MC) surface with ~2–3% crystal boundaries are related to the bio-physical characteristics of the crystalline surface. The unveiling of bio-physical characteristics in terms of crystal boundaries is one of the relevant aspects that provides an understanding of the preferred biological functions, notably, cell adhesion, spread and synthesis of proteins on the NC surface in relation to the MC counterpart.

# **ARTICLE HISTORY**

Received 16 February 2024 Accepted 28 February 2024

#### **KEYWORDS**

Nanocrystalline; crystal boundary; biological functions; bio-physical characteristics

#### Introduction

Stainless steels and titanium alloys are used to fabricate biomedical devices for fixation of hard tissue [1-3]. There are occasions when they fail prematurely because of insufficient build-up of tissue surrounding the biomedical device and/or because of wear. In this context, nanocrystalline (NC) materials are preferred over their microcrystalline (MC) counterpart because the NC surface is considered to promote cellular functionality with the surrounding physiological environment [2]. Furthermore, the increased strength of NC material provides superior wear resistance and is beneficial in ensuring longer life of the biomedical device, besides high strength/weight ratio and correspondingly reduced thickness of the implant. The approach to obtain NC surface in biomedical stainless was recently accomplished using the ingenious phasereversion concept [4–6].

In recent years, biological functions, such as attachment of cells, spreading, mineralization and generation of proteins were studied as a function of crystal size and roughness using different cell lines [7–14]. By revisiting the study on fibroblasts, the primary aim of the present study is to underscore the significance of high fraction of crystal boundaries (>50%) on the NC surface to understand the interaction of fibroblasts with the surface of biomedical stainless steel in terms of bio-physical characteristics and compare it with the MC counterpart.

# **Experimental**

The NC material was obtained from MC austenitic stainless steel using phase-reversion concept developed in the author's laboratory (Figure 1) and is documented in previous studies [4-6,12]. The crystal size depends on the degree of cold deformation of austenite and subsequent temperature-time annealing sequence. The average crystal size of MC and NC austenitic steels was  $22 \pm 3 \,\mu m$  and  $90 \pm 8 \,nm$ (Figure 1), respectively.

MC and NC surfaces were subjected to standard metallography polishing via SiC papers and diamond suspension to almost near-identical nanoscale roughness. The average roughness, Ra, measured from an area of 3  $\mu$ m  $\times$  3  $\mu$ m for MC and NC surface was 1.45  $\pm$  0.21 nm and 1.52  $\pm$  0.29 nm, respectively [4–6,12.

The cell culture protocol for mouse fibroblasts cell line (L-cell-L929; ATCC, U.S.A.) are described in detail earlier [9,14]. Fibroblasts with 80-85% confluence obtained from T-flask cultures by trypsinization were used. In brief, the cells were washed with PBS, incubated with 0.25% trypsin/0.53 mM EDTA for 5 min to detach the cells from Petri dish, dispersed in trypsin/EDTA and centrifuged at 2000 rpm for 5 min. Cell pellet obtained was re-suspended in culture medium, and dilution was carried out using culture medium to obtain the required cell concentration. Subsequently, the sterilized NC and MC samples were placed in 24-well plates and incubated with cell

Figure 1. Light micrograph of MC and TEM micrograph of NC stainless steels [4-6,12].

suspension at 37°C in 5% CO<sub>2</sub> and 95% air atmosphere. Polystyrene 24-well culture plates were used for control experiments [9,14].

## **Results and discussion**

Fluorescent micrographs of fibroblasts (blue spots in Figures 2a,b) [7–9] attached to the NC and MC surfaces indicated greater ability of fibroblasts to attach to the NC surface in relation to the MC surface. This implied that the adhesion of fibroblasts to the surface is influenced by the physical characteristics of the surface and is not influenced by cell development or surface adaptation over time. Cell viability was

measured by mitochondrial reduction of MTT. The observations in Figure 2 clearly suggest that the attachment of fibroblasts was governed by the crystal size.

Intriguingly, the spreading pattern of fibroblasts (Figure 3(i) [7–9] was different on NC and MC surfaces. While the fibroblasts attached and spread well over both the surfaces, but exhibited a different morphology, particularly after 24 h. Fibroblasts cultured on MC surface had a near-round shape, while on the NC surface they were star-shaped with extracellular matrix and cell-to-cell contact. Thus, a significantly greater degree of proliferation of fibroblasts on the NC surface in comparison to the MC surface point towards favourable response and fibroblast cell–surface interaction on the NC surface.

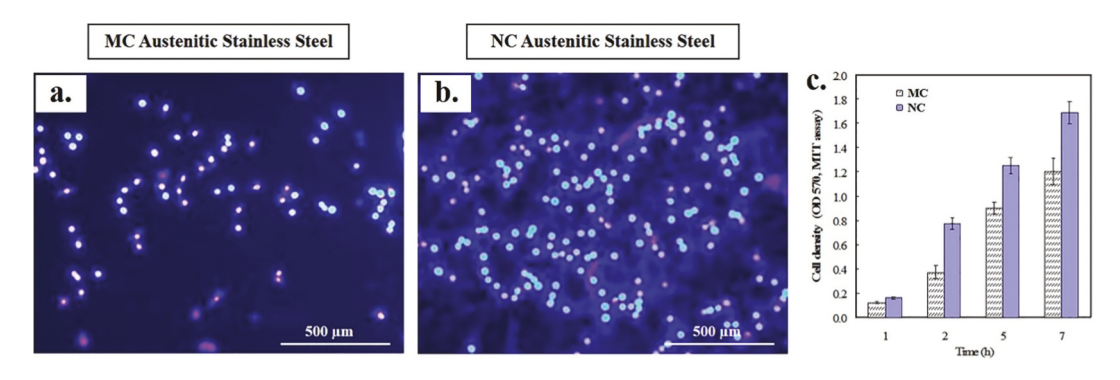


Figure 2. Fluorescence microscopy of fibroblasts nuclei with Hoechst 33,258 after 24 h culture. (a) MC and (b) NC surfaces. NC surface shows higher cell density (b) compared to MC (a) surface. (c) Histograms showing higher initial cell density and viability of fibroblasts on the NC surface using MTT assay [7–9].

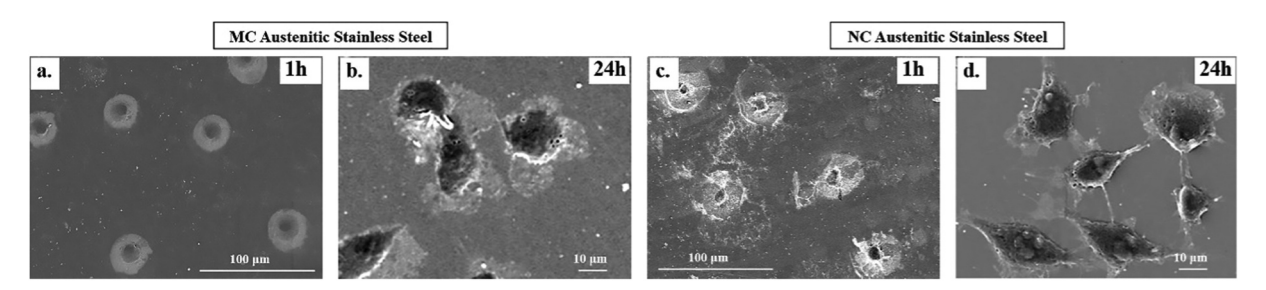


Figure 3(i). SEM micrographs of fibroblasts cultured on MC (a,b) and NC (c,d) surfaces after 1 h (a, c) and 24 h (b, d). Fibroblasts on NC surface after 1 h shows better spreading while cells on MC are round shaped. After 24 h, fibroblasts on NC exhibit extensive spreading and interconnectivity compared to MC surface [7–9].

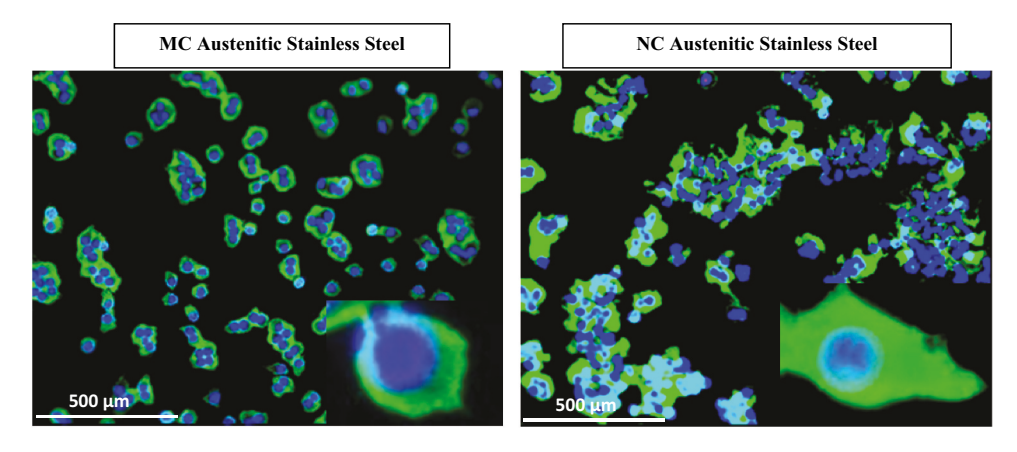


Figure 3(ii). Fluorescence micrographs representing immunocytochemistry of fibronectin by fibroblasts after 2 days on (a) MC and (b) NC surfaces. A higher fluorescence intensity and expanded network of fibronectin expression along with higher cell density is observed after labelling of cell nuclei with DAPI. Inset is the magnified view of the cell [7–9].

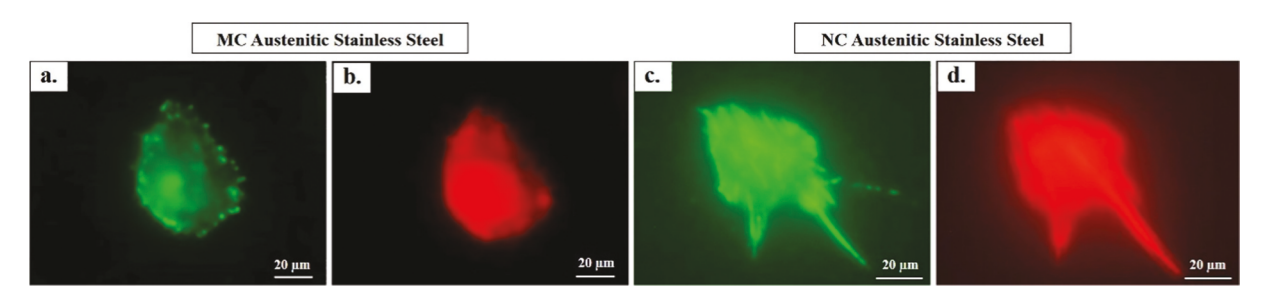


Figure 3(iii). Focal contacts and actin stress fibres after 2 days culture on MC (a, b) and NC (c, d) surfaces. Vinculin (a, c) staining shows a larger number of focal contact sites in fibroblasts grown on NC (c) compared to MC surface (a). The higher number of focal adhesion points correspond well with increased density of actin stress fibres on NC (d) compared to MC surface (b) [7–9].

Examining important proteins, fibronectin, actin, and vinculin, which are linked to cellular functions also indicated that the NC surface was favourable. The degree of expression of key proteins, vinculin and actin that form focal contacts and stress fibres, showed higher expression level and well-defined stress fibres on the NC surface compared to the MC surface (Figure 3(ii, iii)). [7–9].

The briefly described observations lay the foundation and lead us to consider the relationship between the crystal boundaries and cellular functions and define biophysical characteristics in terms of crystal boundaries. Thus, based on the analysis of several micrographs of the type presented in Figures 1, we define average crystal boundary length/surface area of NC and MC surfaces which was  $\sim 15.5 \,\mu\text{m}/\mu\text{m}^2$  and  $\sim 0.14 \,\mu\text{m}/\mu\text{m}^2$ , respectively. Furthermore, the average distance between the crystal boundaries and the dimensions of fibroblasts cells was significantly different for the NC and MC surfaces, if we consider the approximate width of fibroblasts of ~10-20 µm and length of  $\sim 80-100 \,\mu m$ . Thus, on the NC surface, an attached cell covered an average of ~100-200 crystals by width and ~900-1000 crystals by length. While in the case of MC surface, a similar average size of fibroblasts on the MC surface covers

approximately only one or two crystals by width and ~10-15 crystals by length. Thus, the NC surface with several crystal boundaries had a large area covered by the cells (1612 µm<sup>2</sup>) in contrast to the MC surface (984 µm<sup>2</sup>). To explain the observations, bio-physical parameters were defined [15], where the average crystal boundary/cell was combined with cellular functions [15], i.e. average area of NC and MC surface covered by the fibroblasts. The product of these two characteristics provided average crystal boundary length/cell. Table 1 summarizes intriguing results where there is a direct relationship between biophysical characteristics with the interaction of surfaces with the fibroblasts. The average length of crystal boundary/cell occupied by the cells on the NC surface was several times greater than the MC counterpart where the

Table 1. The significance and global contribution of crystal boundaries, bio-physical characteristics and average crystal boundary length/cell for NC and MC surfaces.

	The average area of the surface covered by a fibroblast (µm²)	Average total crystal boundary length/ surface area (μm/μm²)	Average crystal boundary length/cell (μm)
NC	1612.7	15.5	24996
MC	984.5	0.14	138



average intercept length of ~50 nm of the NC surface is similar to the average separation distance of endothelial (~40 nm) [16].

We propose that the high fraction of crystal boundaries on the NC surface provides greater avenue for interactions with the surface through cell signalling and mechano-transduction pathways. This facet is directly related to the features of crystal boundaries, which enhances the interaction of cells with crystal boundaries. Based on the observations described here, it is envisaged that fibroblast cells globally interact with the NC surface in a manner similar to the MC surface. When the cells adhere to the surface, the cells survey the surrounding biological environment and migrate via lamellipodia and filopodia, such that their ends establish focal adhesion. This potentially facilitates consequent transport and communication between fibroblast cells that lead to spreading of cells, synthesis of proteins, and mineralization of extracellular matrix (ECM) by the differentiating fibroblasts.

The findings briefly presented here imply a distinct influence of NC surface on favourable cellular functions. This initiates with greater adhesion of fibroblasts to the NC surface, followed by spreading and synthesis of key proteins. Thus, the enhanced cellular activity on the NC surface can be directly related to the bio-physical parameters (Table 1). We are currently studying other physical, chemical and electronic properties of NC and MC surfaces to develop a phenomenological understanding of the molecular mechanism. For instance, a higher ratio of Cr in the oxide form to that in the metallic form on the NC surface compared to the MC surface is indicative of different electronic properties.

### **Conclusions**

NC surface with the high fraction of crystal boundaries enables significantly enhanced fibroblast cellinteractions, while the interactions of cells with the NC and MC surfaces are similar. This initiates with significantly greater adhesion of cells to the NC surface, which is followed by spreading of cells and synthesis of proteins. Based on the summary of results, it is proposed that crystal boundary bio-physical characteristics govern cellular functions on NC and MC surfaces.

### **Acknowledgments**

The authors are grateful to the National Science Foundation for financial support through grant number CBET 2224942 (Program Manager: Dr. Nora F. Savage).

#### **Disclosure statement**

No potential conflict of interest was reported by the author(s).

## **Funding**

This work was supported by the National Science Foundation [CBET 2224942].

#### References

- [1] Borsari V, Giavaresi G, Fini M, et al. Physical characterization of different-roughness titanium surfaces, with and without hydroxyapatite coating, and their effect on human osteoblast-like cells. J Biomed Mater Res. 2005;75B(2):359. doi: 10.1002/jbm.b.30313
- Balasundaram G, Webster T. Increased osteoblast adhesion on nanograined Ti modified with KRSR. J Biomedical Materials Res. 2007;80A(3):602. doi: 10. 1002/jbm.a.30954
- [3] Willman G. Coating of implants with hydroxyapatite material connections between bone and metal. Adv Eng Mater. 1999;1(2):95. doi: 10.1002/(SICI)1527-2648 (199910)1:2<95:AID-ADEM95>3.3.CO;2-G
- [4] Misra RDK. Scientific reports. Nature. 2018;8 (7908):1-13.
- [5] Misra RDK, Challa VSA, Venkatsurya PKC, et al. Interplay between grain structure, deformation mechanisms and austenite stability in phase-reversion-induced nanograined/ultrafinegrained austenitic ferrous alloy. Acta Materialia. 2015;84:339. doi: 10.1016/j.actamat. 2014.10.038
- [6] Misra RDK, Nayak S, Venkatasurya PKC, et al. Nanograined/ultrafine-grained structure and tensile deformation behavior of shear phase reversioninduced 301 austenitic stainless steel. Metal And Matls Trans A. 2015;41 A:2162-2174. doi: 10.1007/ s11661-010-0230-6
- [7] Misra RDK, Thein-Han WW, Pesacreta TC, et al. Favorable modulation of pre-osteoblast response to nanograined/ultrafine-grained structures in austenitic stainless steel. Adv Mater. 2009;21(12):1280. doi: 10. 1002/adma.200802478
- [8] Misra RDK, Thein-Han WW, Pesacreta TC, et al. Cellular response of preosteoblasts to nanograined/ ultrafine-grained structures. Acta Biomaterialia. 2009;5(5):1455. doi: 10.1016/j.actbio.2008.12.017
- [9] Misra RDK, Thein-Han WW, Pesacreta TC, et al. Biological significance of nanograined/ultrafinegrained structures: interaction with fibroblasts. Acta Biomaterialia. 2010;6(8):3339. doi: 10.1016/j.actbio. 2010.01.034
- [10] Misra RDK, Thein-Han WW, Mali SA, et al. Cellular activity of bioactive nanograined/ultrafine-grained materials. Acta Biomaterialia. 2010;6(7):2826. doi: 10. 1016/j.actbio.2009.12.017
- [11] Venkatsurya PKC, Thein-Han WW, Mali SA, et al. Cellular activity of bioactive nanograined/ultrafinegrained materials. Acta Biomaterialia. 2010;6 (7):2826. doi: 10.1016/j.actbio.2009.12.017
- [12] Misra RDK, Challa VSA, Injeti VSY, et al. Phase reversion-induced nanostructured austenitic alloys: an overview. Mater Technol. 2022;37(7):437. doi: 10. 1080/10667857.2022.2065621

- [13] Nune KC, Montes I, Injeti VSY, et al. The determining role of nanoscale mechanical twinning on cellular functions of nanostructured materials. J Mech Behav Biomed Mater. 2018;88:185. doi: 10.1016/j.jmbbm. 2018.08.033
- [14] Misra RDK, Thein-Han W-W, Somani MC, et al. Phase reversion-induced nanograined/ultrafine-grained structures in austenitic stainless steel and their significance in modulating cellular response: biochemical and morphological study
- with fibroblasts. Adv Eng Mater. 2009;11(12): B325. doi: 10.1002/adem.200900164
- [15] Lowe TC, Reiss RA, Illescas PE, et al. Effect of surface grain boundary density on preosteoblast proliferation on titanium. Mater Res Lett. 2020;8(6):239. doi: 10. 1080/21663831.2020.1744758
- [16] Le Saux G. Le Hezbollah libanais et la résistance islamique au Liban : des stratégies complémentaires. Confluences Méditerranée. 2011; N° 76(1):101-111. doi: 10.3917/come.076.0101